

First-Principles Investigation of Ru- and Pt-Doped TiO₂ Brookite Surfaces

Ratshilumela Steve Dima^{1,2}, Nditsheni Eric Maluta^{2,*} and Rapela Regina Maphanga^{1,3}

¹ Council for Scientific and Industrial Research, Next Generation Enterprises and Institution Cluster, P.O Box 395, Pretoria, 0001, South Africa.

² University of Venda, Department of Physics, P/Bag X 5050, Thohoyandou, 0950, South Africa

³ University of Limpopo, Department of Physics, Private Bag X 1106, Sovenga, 0727, South Africa.

*E-mail: eric.maluta@univen.ac.za

Received: 31 May 2019 / *Accepted:* 31 October 2019 / *Published:* 31 December 2019

The electronic structures and optical properties of brookite TiO₂ (100) and (110) surfaces doped with transition metals (Ru and Pt) have been investigated by first-principles calculations based on the density functional theory, employing generalized gradient approximation (GGA). The modelled surface structures were constructed from an optimized brookite bulk structure. TiO₂ surfaces were doped with transition metals, with one Ti atom replaced by a transition metal atom. The results indicate that doping with both transition metals can narrow the band gap of TiO₂, leading to the improvement in the photo reactivity of TiO₂. The metal dopants shift the absorption to high wavelengths and improves optical absorbance in the visible and near-IR region. The surface (100) showed higher activity than (110) in both regions.

Keywords: Density functional theory; TiO₂; brookite; dye sensitized solar cell; doping

1. INTRODUCTION

Since the invention of dye-sensitized solar cells (DSSCs) in 1991, there has been extensive research on DSSCs as alternatives to silicon-based solar cells, owing to their simple structure, transparency, flexibility, low production cost and wide range of applications. Despite the advantages of DSSCs, their low efficiency compared to that of silicon-based cells has limited their commercial application [1-4]. Consequently, there is a real need to improve the efficiency of DSSCs in order to realize next-generation solar cells. Titanium dioxide exists in various forms amongst which rutile and anatase polymorphs have been extensively studied owing to their great potential for a wide range of applications, such as photocatalysis [5-9] and low-cost solar cells [1-7]. Studies and experimental data

on brookite polymorph of TiO_2 is limited due to its scarcity and more difficulty synthesis [10]. TiO_2 being a non-toxic, environmentally benign, low-cost semiconductor with long-term stability, it is one of the foremost materials for photovoltaic applications. However, the potential for various applications is limited by the wide band gap of TiO_2 polymorphs (rutile 3.0 eV, anatase 3.2 eV and brookite 3.4 eV) [11, 12], which confine their photoactivity to the ultraviolet region of the electromagnetic spectrum i.e. $< 5\%$ for photocatalytic oxidation. Effective utilization of visible light, which constitutes $> 45\%$ of the solar irradiance is highly important to significantly widen the avenue to use TiO_2 in DSSCs [13, 14]. TiO_2 material can be used indirectly as an electron-transporting substrate for chemisorbed photoactive dye in technically and economically viable DSSCs. The charge-carrier transport in DSSC is based on light absorption by the dye molecules anchored onto TiO_2 nanoparticles, followed by the transfer of electrons into the wide band gap of the TiO_2 and through the transparent conducting oxide to the external load.

To overcome the UV limitation, many efforts have been devoted to extending the spectral response of TiO_2 to visible light; this included energy band modulation by doping TiO_2 matrix with various transition metal ions [15-23] and non-metals [24-32]. Doping with transition metals is regarded as one of the most effective approaches to extend the absorption edge of TiO_2 to visible light due to their unique electronic d-configuration and spectral characteristics, which provide defect states in the band gap [12, 22, 26, 33]. The doping with different atoms within certain limits in any material framework extends the lifetime of charge carriers if the dopants have energy levels just below the conduction band or above the valence band, thus acting as charge carrier trapping centers and also extending their wavelength response towards the visible region. Metals such as Fe, Cr, Co, Mo and V have been used to tune the electronic structure and enhance the photocatalytic activity of TiO_2 [16, 22]. Choi [22] reported the highest chloroform degradation efficiency under UV irradiation for a sample containing 0.5% Fe^{3+} and the substitution of Ti^{4+} ions in TiO_2 . Umabayshi [16] showed that the localized energy levels due to Co doping are sufficiently low to lie at the top of the valence band, while dopants such as V, Mn, Fe, Cr and Ni produced mid-gap states [16].

Several density functional theory (DFT)-based studies on various TiO_2 phases (mostly rutile and anatase) have been published to date [8, 34-38]. The more complex brookite phases, with symmetry-reduced structures are affected by increasing disorder and may have interesting optical properties, although sufficient evidence is still missing. The aim of this paper is to understand doping mechanisms and band gap engineering, by investigating structural, electronic and optical properties of ruthenium and platinum-doped TiO_2 brookite surfaces through density functional theory.

2. COMPUTATIONAL METHOD

The DFT calculations were performed with the plane wave pseudopotential method to determine the structural, electronic and optical properties of doped and un-doped TiO_2 (100) and (110) surfaces. The generalized gradient approximation in the scheme of Perdew-BurkeErnzerhof (PBE) was used to describe the exchange-correlation functional. All calculations were done using CASTEP code in Materials Studio of BIOVIA Inc [39, 40].

The convergence test showed that the cut-off kinetic energy of plane waves was 650 eV. The Brillouin zone k-point sampling was performed using a Monkhorst Pack mesh, 4x4x2. The convergence criteria for structural optimization were set to be medium quality with the tolerance for self-consistent field (SCF), energy, maximum force, and maximum displacement of 2.0106 eV/atom, 2.0105 eV/atom, 0.05 eV/atom and 2.0103 eV/atom, respectively.

The surface structures of TiO₂ brookite were constructed from unreconstructed bulk structure slab model employing the calculated equilibrium geometry. All surface slab models featured 10 Å vacuum thickness, but each had a different crystal thickness due to different atom orientations. These surfaces had different number of atoms in each layer, therefore, after the relevant convergence tests, the surfaces were periodically modelled in the *x*- and *y*-directions but with a different thickness in the *z*-direction. The relaxation of these surfaces was considered by optimizing all the layers of the slab. The surfaces were doped by replacing one Ti atom with a Ru/Pt atom (substitutional doping).

3. RESULTS AND DISCUSSIONS

3.1. Structural Properties

Brookite TiO₂ is known to have a complex structure, consisting of eight formula units in the orthorhombic cell with space group Pbca. The formation of the brookite structure may be envisioned as the joining of a distorted TiO₆ octahedral sharing three edges. Figure 1 illustrates the bulk structure of brookite TiO₂.

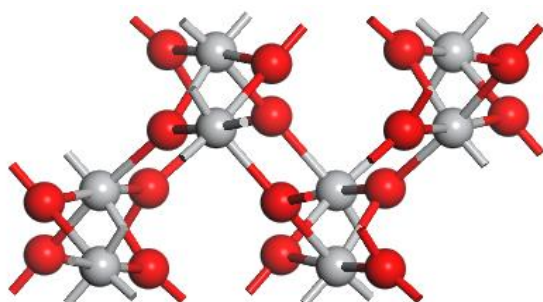


Figure 1. The bulk structure of TiO₂ brookite. The grey spheres represent Ti-atoms while red spheres represent O-atoms.

The truncation of the octahedral renders different coordination combinations for the outermost titanium cations. Depending on the orientation of the brookite surface, the surface was either oxygen or titanium terminated. However, the effect of surface termination was not investigated in detail in this study as the focus was on understanding the effect of doping with Ru and Pt. All the brookite surface structures were optimized by relaxing surface atoms to eliminate surface atomic tension. The dopants were introduced by replacing one Ti-atom with a Ru or Pt atom.

Figure 2 shows the structures of the un-doped and doped brookite (100) surfaces. The atomic surface underwent relaxation, but not reconstruction. For all the brookite (100) surfaces, the top and bottom layers of oxygen ions are 2-fold coordinated (O_{2c}), with the nearest titanium ions being 4-fold coordinated (Ti_{5c}).

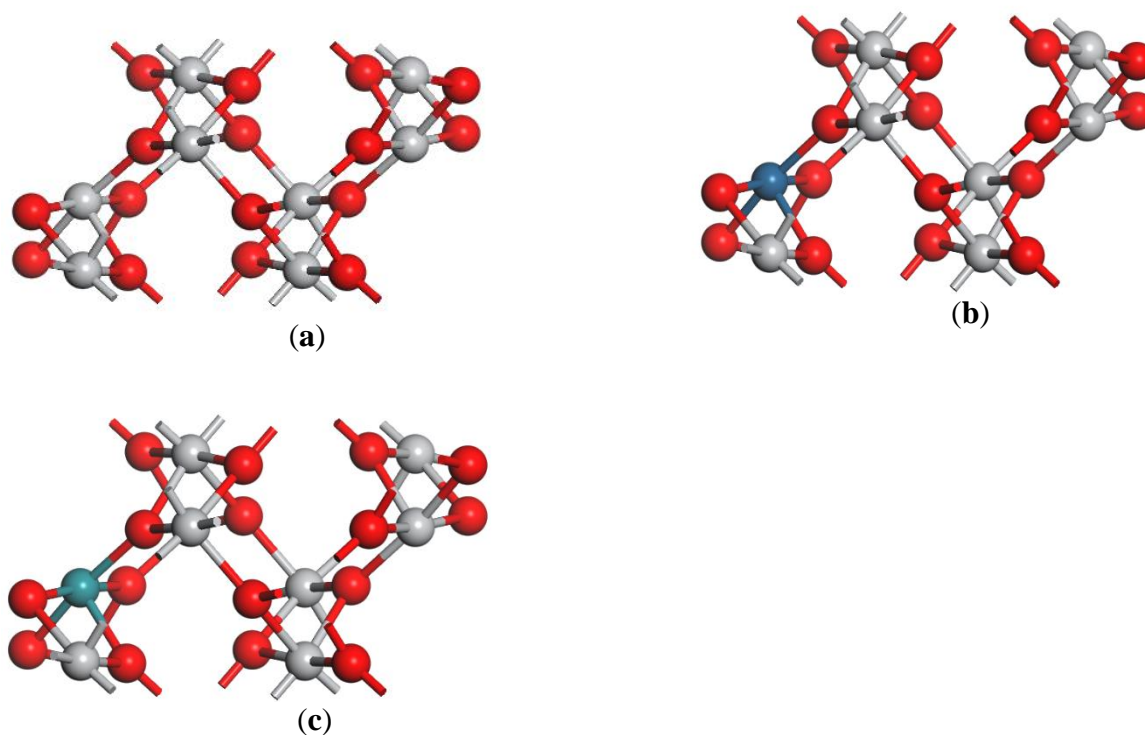


Figure 2. Atomic structures of brookite TiO_2 (100) surface: (a) un-doped TiO_2 , (b) Ru-doped brookite TiO_2 , (c) Pt-doped brookite TiO_2 . The grey, red, green and blue spheres represent Ti-atoms, O-atoms, transition metal Ru and Pt respectively.

Figure 3 shows the atomic structures of brookite TiO_2 (110) surfaces for both un-doped and doped systems. The ideal (110) brookite surface is known to be characterized by the presence of pairs of coordinative unsaturated ions, i.e., 6-fold coordinated Ti (Ti_{6c}) and two types of 2-fold coordinated oxygen ions (O_{2c} , O'_{2c}); each of these atoms consists of one cleaved bond. The ideal (110) brookite surface also consists of some 3-fold coordinated O (O_{3c}) and 5-fold coordinated Ti (Ti_{5c}) [41]. The brookite TiO_2 (110) surface structure has a mixture of Ti and O termination. The dopants were introduced by replacing one 6-fold Ti atom with a Ru or Pt atom.

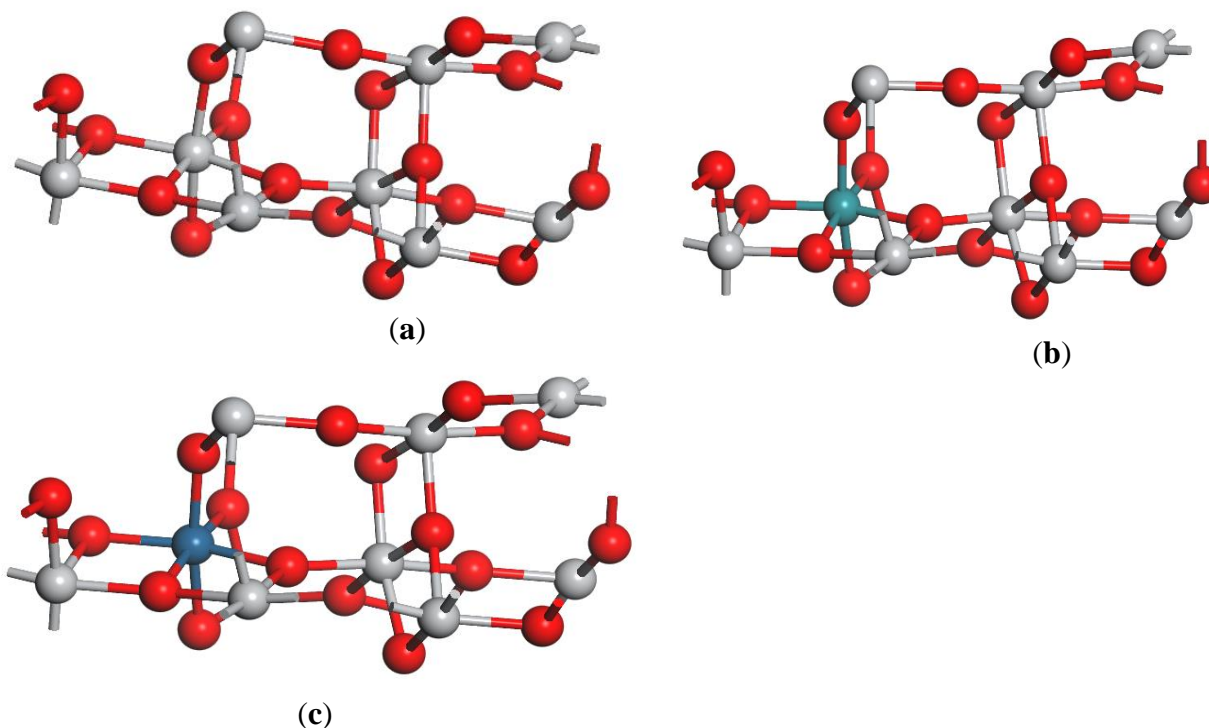


Figure 3. Atomic structures of brookite TiO_2 (110) surfaces (a) un-doped TiO_2 , (b) Ru doped brookite TiO_2 , (c) Pt doped brookite TiO_2 . The grey, red, green and blue spheres represent Ti-atoms, O-atoms, transition metal atoms Ru and Pt respectively.

3.2. Electronic properties

3.2.1. Un-doped surface structure

The band structure of brookite TiO_2 was constructed in the appropriate high-symmetry directions of the relevant irreducible Brillouin zone using the calculated lattice parameters. The band structure and density of states (DOS) near the Fermi energy of the bulk TiO_2 are presented in Figure 4. The calculated energy band gap of the bulk brookite TiO_2 was found to be 2.353 eV. The band gap value is comparable to that reported by Mo and Ching [12], obtained using the self-consistent orthogonalized linear combination of atomic orbitals method. Both the conduction band minimum (CBM) and the valence band maximum (VBM) are located at G. Thus, brookite TiO_2 is a direct band gap semiconductor. The upper valence band (VB) consists of O 2p states and the bottom of the conduction band (CB) consists of Ti 3d states. According to Mo and Ching, brookite TiO_2 has a direct band gap of 2.20 eV. The calculated band gap and that reported by Mo and Ching were found to be underestimated compared with the experimentally measured value of 3.40 eV; this is due to the limitation of DFT [11, 12]. The limitation is caused by the discontinuity in the exchange-correlation potential, which is not considered within the framework of DFT. For this work, the scissor operation of 1.047 eV was employed to compensate for the underestimation of the band gap. The scissors scheme aligns both the theoretical valence band energy (VBE) and conduction band energy (CBE) with their corresponding experimental results, by performing

a scissor operation to widen out the theoretical band gap states over the experimental band gap. The experimental value used for the scissor operation was 3.40 eV, a value that was reported by Koelsch [11]. After the scissor operation, the band gap value became 3.40 eV as shown in Figure 4.

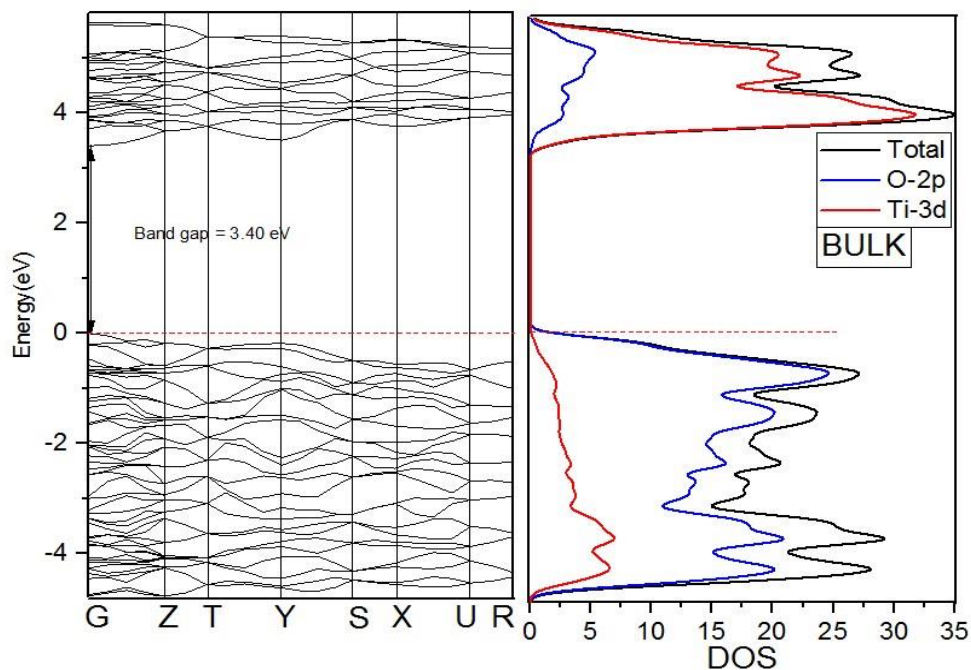


Figure 4. Band structure (left) and density of state (right) for un-doped bulk brookite TiO_2 .

The calculated band gaps of undoped (100) and (110) brookite TiO_2 surfaces are 3.350 eV and 4.570 eV respectively, as shown in Figure 5 (a) and (b). The band gaps for the surface structures are larger than that of the bulk system. These results indicate that the distribution probability of the electron is biggest in the surface, i.e. the electron is limited near the surface. This type of electronic state is called the surface state and the related energy levels are called the surface levels. Figures 5 (a) and (b) show that there are no surface levels appearing near the Fermi level, which indicates that there are no surface states within the framework of the material.

The results indicate that the valence band of the pure brookite TiO_2 surfaces mainly consists of the hybridization of O 2p and Ti 3d states whereas the conduction band is mainly composed of Ti 3d states demonstrating consistency with the experimental results [11]. The O 2p and Ti 3d states show resonance phenomenon, indicating that some covalence bond character between titanium and oxygen atoms exist in agreement with previous studies [12].

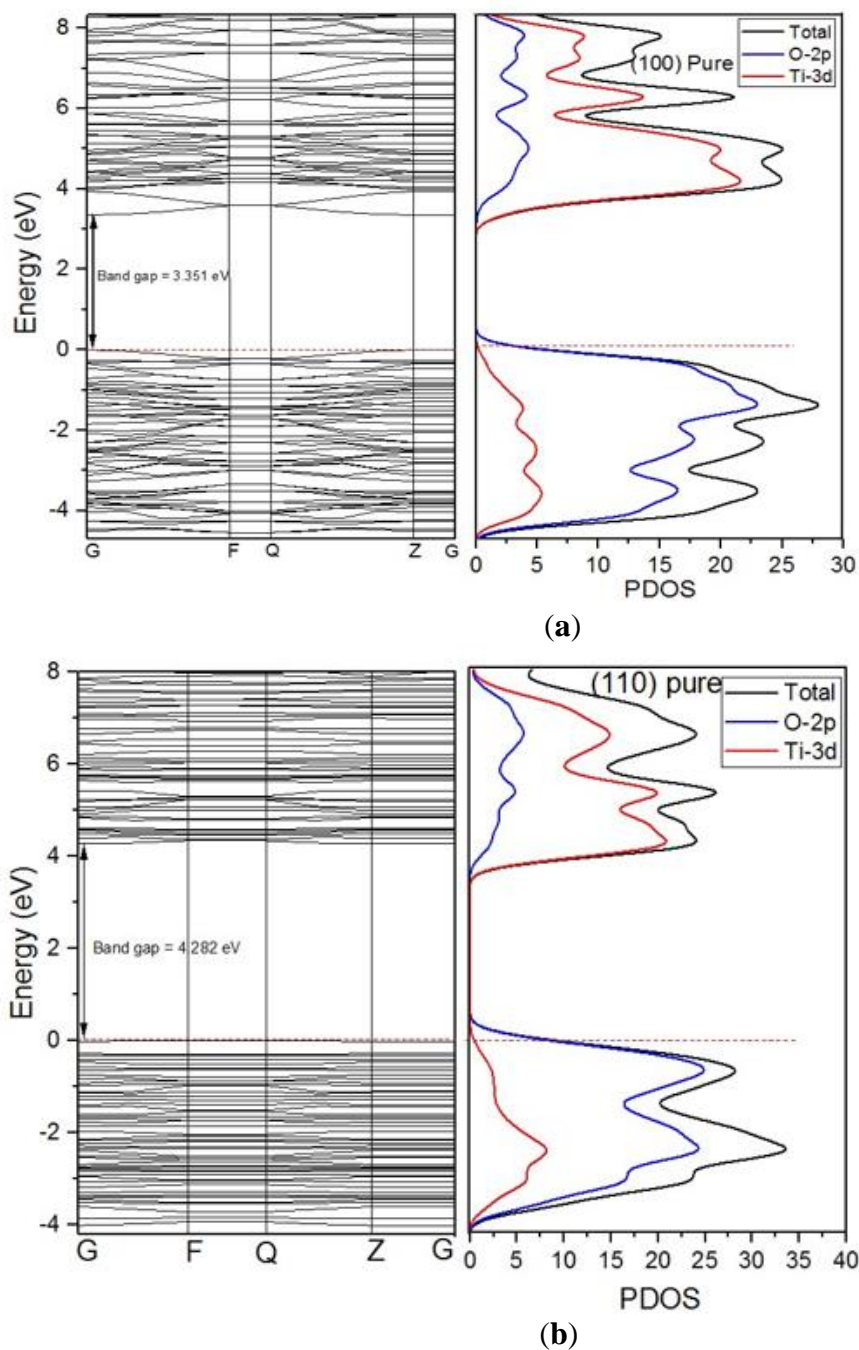


Figure 5. Band structure (left) and density of states (right) for un-doped bulk brookite TiO_2 (a) (100) and (b) (110) surfaces.

3.2.2. Doped surface structure

The total density of states (TDOS) and partial density of states (PDOS) of Ru-doped brookite TiO_2 (100) and (110) surfaces are shown in Figures 6 (a) and (b). The TDOS shape of transition metal-doped TiO_2 in both the VB and CB are broader than that of pure TiO_2 , indicating that the electronic nonlocality is more obvious, due to the reduction of crystal symmetry.

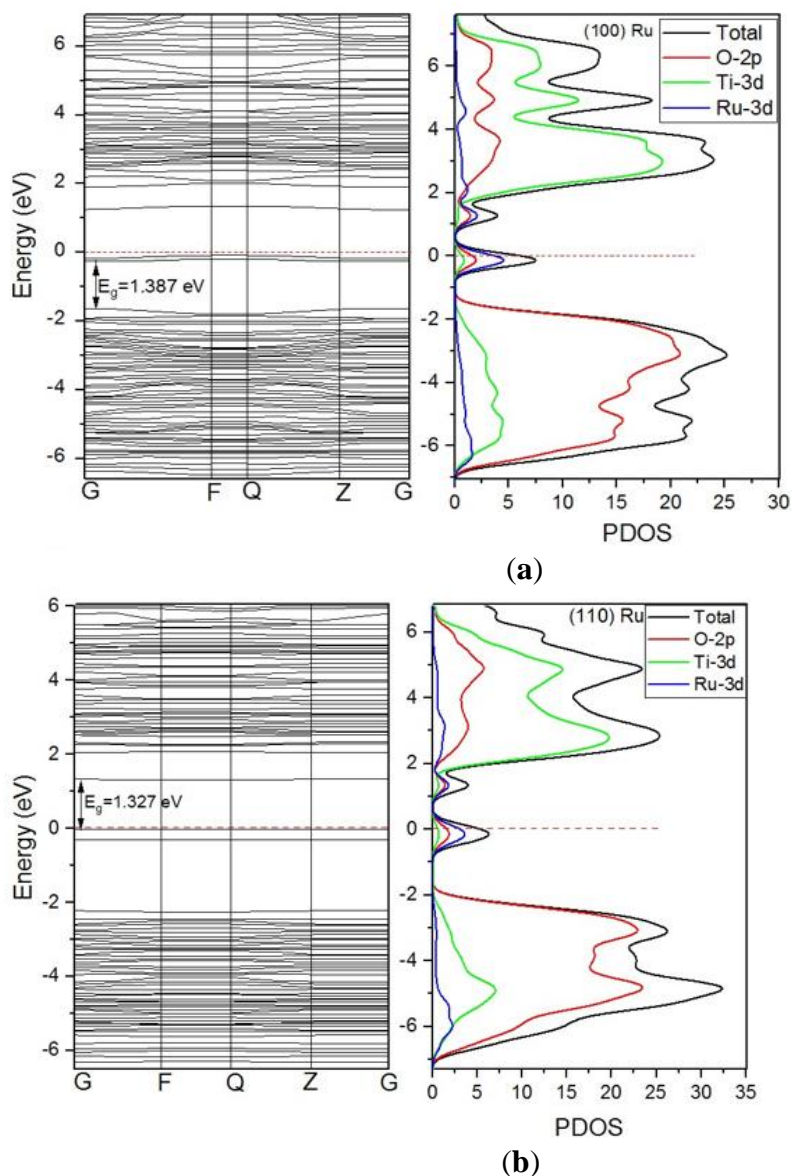


Figure 6. Band structure (left) and density of states (right) for undoped bulk brookite TiO_2 (a) (100) and (b) (110) surfaces.

The 3d-state of dopant transition metals are delocalized to some moderate extent, which gives rise to the formation of impurity energy levels (IELs) through hybridization with O 2p or 3d Ti states. These IELs formed by the hybrid effect can form mid band gap or within the valence band and conduction band, which provides a trapping potential well for the electrons and holes. These IELs contribute to the separation of photo-generated electron hole pairs, and work in favour of the migration of photo-excited carriers and the process of photocatalysis process. For the brookite TiO_2 (100) surface doped with Ru, the PDOS reveal that Ru 3d states seem to be isolated IELs located just below the bottom of the conduction band near the Fermi level, with one of them completely occupied and the others unoccupied. These IELs overlap with conduction band minimum of TiO_2 surfaces. This type of doping is called n-type doping, which results from the fact that the impurity has more valence electrons than the host as seen in the band structure plot in Figure 6 (a). Thus, the band gap of Ru-doped brookite TiO_2 (100) surface was determined to be 1.387 eV.

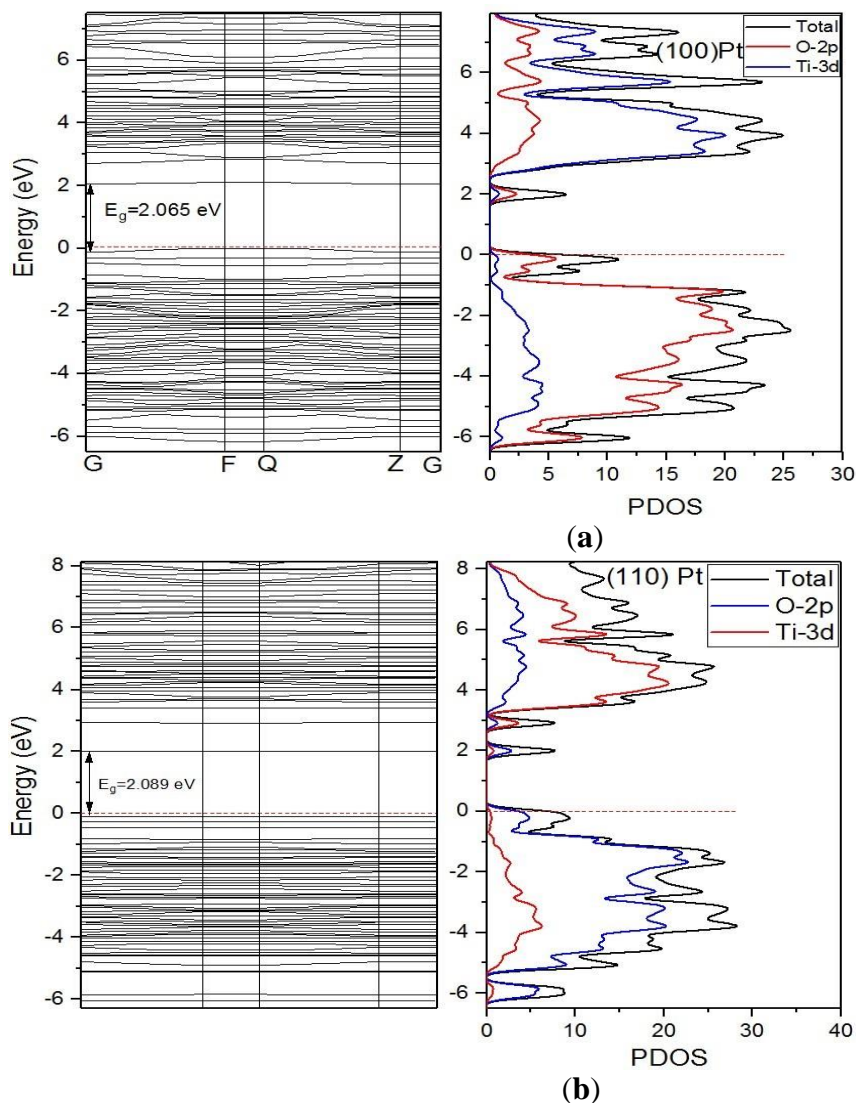


Figure 7. Band structure and density of states of Pt-doped brookite TiO_2 (a) (100) and (b) (110) surfaces.

Similarly, the (110) brookite TiO_2 PDOS reveal that Ru 3d states appear as isolated IELs located below the bottom of the conduction band with one of them completely occupied and the others unoccupied. These IELs sufficiently overlap with conduction band minimum of TiO_2 surfaces, which is a p-type doping owing to fact that the impurity has fewer valence electrons than the host as shown in the band structure given in Figure 6(b). The band gap for Ru-doped (110) brookite TiO_2 surface was found to be 1.327 eV. It is worth noting that the band gap of Ru-doped brookite TiO_2 surfaces is not associated with the gap between the Ti t_{2g} (d_{xy} , d_{xz} , d_{yz}) and e_g (d_{z^2} , $d_{x^2-y^2}$) bands, but is related to the energy separation between the O 2p and the Ti t_{2g} bands of TiO_2 , which are modified by dopant atoms.

The TDOS and PDOS for Pt-doped (100) and (110) surfaces presented in Figure 7 (a) and (b) indicate that there is a single Pt 6c situated at the hollow site and interacting with Ti 5c that appears as a PtTi 5c hybridization peak at the bottom of the CB. There are four occupied flat gap states just above the VB near the Fermi level; these result from the non-bonding excess charges around Pt. For Ru-doped TiO_2 , the PDOS calculation corresponding to Ru 3d show new IELs located above the top of the valence

band. In contrast to Ru-doped surfaces, Pt 5d states in the Pt-doped (110) surface are somewhat delocalized. The valence band is composed mainly of the O 2p states, with the IELs located just above the top of valence band. They are formed by hybridization of O 2p states and Ti 3d states with 5 d9 6 s1 states. When the IELs are considered, the CBM is located at approximately -2.0 eV, the width of CB is approximately 3.9 eV, and the width of VB is approximately -6.2 eV. Compared to un-doped surface, the band gap of Pt-doped TiO₂ narrowed to 2.065 eV for (100) surface and 2.089 eV for (110) surface, due to the mixing of Pt 5 d9 6 s1 states with O 2p states and Ti 3d broadening the width of the valence band.

3.3. Optical Properties

The polarized model of TiO₂ was used to calculate the absorption spectra of the various surface systems. The optical calculations were based on the ground state of the electrons. The calculated UV-Vis absorption spectra for un-doped as well Ru- and Pt-doped TiO₂ (100) and (110) surfaces are shown in Figure 8 (a) and (b) respectively

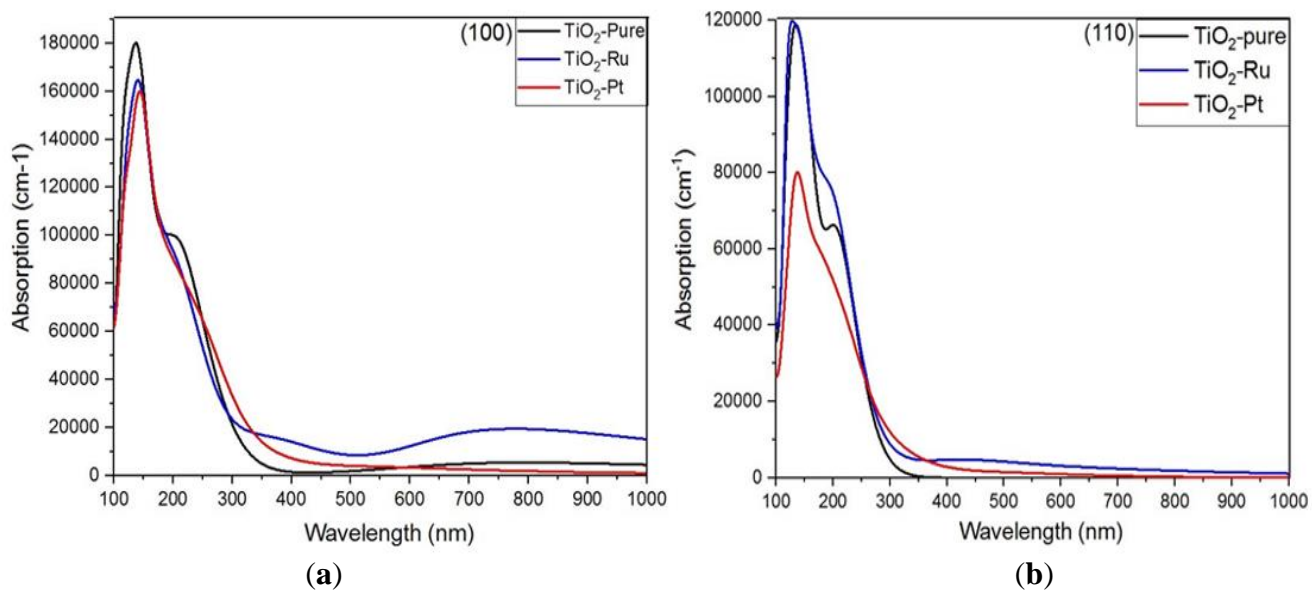


Figure 8. Optical absorption curves of the un-doped and doped brookite TiO₂ (a) (100) and (b) (110) surfaces.

According to literature, due to the intrinsic wide band gap, pure brookite TiO₂ can only show photocatalytic activity under ultraviolet light irradiation, which indicates that there is a limited range of involvement of the semi-conducting material in DSSCs and photoelectrochemical cells [42, 43]. Figures 8(a) and 8(b) show that, after doping, the electronic structure's composition change and the optical absorption edge shift to the visible light region. From the (100) surface, it was observed that there is a slightly smaller decrease in the absorption coefficient of Ru-TiO₂ and Pt-TiO₂ in the ultraviolet region of the spectrum in comparison to that of the pure brookite TiO₂. However, in the case of the (110) surface, only Ru-TiO₂ showed a decrease in the absorption coefficient in the ultraviolet region of the spectrum. The Ru-doped surface has the greatest red shift as shown in Figure 8 by a high peak absorbing from 400 nm towards the infrared (IR) region. The red shift may be caused by IELs. Pt-doped surfaces

showed less absorption capability than the un-doped surface at 700 nm in (100) surface. This revealed that Pt doping in the (100) surface is more effective in the lower part of the visible region of the spectrum. In the case of the (110) surface, Ru-doped TiO₂ had the greatest absorption peak in the visible and IR region of the spectrum. Pt-doped TiO₂ surface also showed some activity in both the visible and IR region. Ru-doped surface shows higher absorption or activity than the un-doped surface throughout the visible and the IR region. The overall analyses of the UV–Vis absorption spectra revealed that doping the systems with Ru or Pt not only increases efficiency of energy absorption, thus promoting electron transition, but also strengthens the absorption capacity of visible light. In addition, both Ru and Pt doping largely improve photocatalytic activity of TiO₂ in the visible light region; this is in agreement with previous studies on rutile TiO₂ [44]. With these optical properties, the doped systems are great candidates for use as semiconducting materials in DSSCs and photoelectrochemical cells which require a semiconductor that has a high absorption coefficient in the visible region, extending to the IR region of the spectrum.

4. CONCLUSIONS

First-principle calculations were successfully used to investigate electronic and optical properties of un-doped and Ru- or Pt-doped brookite TiO₂ (100) and (110) surfaces. The two low index surfaces of brookite TiO₂, i.e. (100) and (110) surfaces were generated by cleaving the optimized bulk structure. The study revealed that truncation of the octahedral give different coordination combinations for the outermost Ti-cations. All the surfaces were characterized by the presence of two types of 2-fold coordinated O-atoms (O_{2c} and O'2c) and 5-fold and 6-fold coordinated Ti-atom (Ti_{5c} and Ti_{6c}). Doping TiO₂ surfaces with Ru or Pt showed a subtle atomic rearrangement for all the surfaces. Based upon calculated results, the analysis of electronic structures suggests that metal dopants shift the VB to higher energy for all the surfaces. The results also indicate that the spectrum wavelength of the material may be extended to the visible light region and near-infrared region. This can be observed from the formation of the IELs, which are mainly hybridized by 3d and 5d states of impurities with O 2p states or Ti 3d states. The components of electronic properties and dopant states from the band structures and the TDOS support the fact that metal dopants are active in the inter-band and mid-gap state transitions induced by lower energy excitations, which are important for the application of solar energy conversion. The compensating optical absorbance of Ru- or Pt-dopants in different wavelength regions imply that both dopants may possess prominent optical absorption properties. Theoretical research on transition metal brookite TiO₂ provides significant evidence for developing the photocatalytic applications. Theoretical calculation of doped TiO₂ is however still an ongoing exercise, and there are a few challenges which require further investigation to enable optimal performance and application of these materials in DSSCs.

ACKNOWLEDGMENTS

The authors would like to acknowledge Centre for High Performance Computing (CHPC) for computing resources.

References

1. B. O'regan and M. Grätzel, *Nature*, 353 (1991) 737.
2. B.-K. Lee and J.-J. Kim, *Current Applied Physics*, 9 (2009) 404.
3. B. O'Regan, M. Grätzel, and D. Fitzmaurice, *Chemical Physics Letters*, 183 (1991) 89.
4. M. Dürr, A. Schmid, M. Obermaier, S. Rosselli, A. Yasuda, and G. Nelles, *Nature Materials*, 4 (2005) 607.
5. A. Fujishima and K. Honda, *Nature*, 238 (1972) 37.
6. M. R. Hoffmann, S. T. Martin, W. Choi, and D. W. Bahnemann, *Chemical Reviews*, 95 (1995) 69.
7. A. Kay and M. Grätzel, *Solar Energy Materials and Solar Cells*, 44 (1996) 99.
8. F. M. Hossain, L. Sheppard, J. Nowotny, and G. E. Murch, *Journal of Physics and Chemistry of Solids*, 69 (2008) 1820.
9. X. Chen and C. Burda, *Journal of the American Chemical Society*, 130 (2008) 5018.
10. A. Di Paola, M. Bellardita, and L. Palmisano, *Catalysts*, 3 (2013) 36.
11. M. Koelsch, S. Cassaignon, J. Guillemoles, and J. Jolivet, *Thin Solid Films*, 403 (2002) 312.
12. S.-D. Mo and W. Ching, *Physical Review B*, 51 (1995) 13023.
13. R. Dima, N. Maluta, R. Maphanga, and V. Sankaran, *Journal of Physics: Conference Series* (2017) 012012.
14. V. Binas, D. Venieri, D. Kotzias, and G. Kiriakidis, *Journal of Materiomics*, 3 (2017) 3.
15. F. De Angelis, S. Fantacci, A. Selloni, M. K. Nazeeruddin, and M. Grätzel, *The Journal of Physical Chemistry C*, 114 (2010) 6054.
16. T. Umabayashi, T. Yamaki, H. Itoh, and K. Asai, *Journal of Physics and Chemistry of Solids*, 63 (2002) 1909.
17. A. Di Paola G. Marci, L. Palmisano, M. Schiavello, K. Uosaki, S. Ikeda, and B. Ohtani, *The Journal of Physical Chemistry B*, 106 (2002) 106.
18. S.-m. Chang and R.-a. Doong, *The Journal of Physical Chemistry B*, 110 (2006) 20808.
19. Y. Segura, L. Chmielarz, P. Kustrowski, P. Cool, R. Dziembaj, and E. Vansant, *The Journal of Physical Chemistry B*, 110 (2006) 948.
20. B. Jongsomjit, T. Wongsalee, and P. Praserttham, *Catalysis Communications*, 6 (2005) 705.
21. K. Wilke and H. Breuer, *Journal of Photochemistry and Photobiology A: Chemistry*, 121 (1999) 49.
22. W. Choi, A. Termin, and M. R. Hoffmann, *The Journal of Physical Chemistry*, 98 (1994) 13669.
23. D. Dvoranova, V. Brezova, M. Mazúr, and M. A. Malati, *Applied Catalysis B: Environmental*, 37 (2002) 91.
24. S. U. Khan, M. Al-Shahry, and W. B. Ingler, *Science*, 297 (2002) 2243.
25. S. Sakthivel and H. Kisch, *Angewandte Chemie International Edition*, 42 (2003) 4908.
26. J. C. Yu, J. Yu, W. Ho, Z. Jiang, and L. Zhang, *Chemistry of Materials*, 14 (2002) 3808.
27. T. Umabayashi, T. Yamaki, S. Yamamoto, A. Miyashita, S. Tanaka, T. Sumita and K. Asai, *Journal of Applied Physics*, 93 (2003) 5156.
28. O. Diwald, T. L. Thompson, T. Zubkov, E. G. Goralski, S. D. Walck, and J. T. Yates, *The Journal of Physical Chemistry B*, 108 (2004) 6004.
29. M. Miyauchi, A. Ikezawa, H. Tobimatsu, H. Irie, and K. Hashimoto, *Physical Chemistry*, 6 (2004) 865.
30. N. C. Saha and H. G. Tompkins, *Journal of Applied Physics*, 72 (1992) 3072.
31. J. He, J. Zhao, T. Shen, H. Hidaka, and N. Serpone, *The Journal of Physical Chemistry B*, 101 (1997) 9027.
32. A. Hattori, M. Yamamoto, H. Tada, and S. Ito, *Chemistry Letters*, 27 (1998) 707.
33. K. M. Glassford and J. R. Chelikowsky, *Physical Review B*, 46 (1992) 1284.
34. M. Landmann, E. Rauls, and W. Schmidt, *Journal of Physics: Condensed Matter*, 24 (2012) 195503.

35. N. H. Vu, H. V. Le, T. M. Cao, V. V. Pham, H. M. Le, and D. Nguyen-Manh, *Journal of Physics: Condensed Matter*, 24 (2012) 405501.
36. Z.-P. Liu, X.-Q. Gong, J. Kohanoff, C. Sanchez, and P. Hu, *Physical Review Letters*, 91 (2003) 266102.
37. J. Muscat, V. Swamy, and N. M. Harrison, *Physical Review B*, 65 (2002) 224112.
38. X. Wu, E. Holbig, and G. Steinle-Neumann, *Journal of Physics: Condensed Matter*, 22 (2010) 295501.
39. A. R. Albuquerque, M. L. Garzim, I. d. M. d. Santos, V. Longo, E. Longo, and J. R. Sambrano, *The Journal of Physical Chemistry A*, 116 (2012) 11731.
40. S. J. Clark, M. D. Segall, C. J. Pickard, P. J. Hasnip, M. J. Probert, K. Refson and M. C. Payne, *Zeitschrift Fuer Kristallographie*, 220 (2005) 567.
41. A. Beltran, L. Gracia, and J. Andres, *The Journal of Physical Chemistry B*, 110 (2006) 23417.
1. B. O'regan and M. Grätzel, *Nature*, 353 (1991) 737.
2. B.-K. Lee and J.-J. Kim, *Current Applied Physics*, 9 (2009) 404.
3. B. O'Regan, M. Grätzel, and D. Fitzmaurice, *Chemical Physics Letters*, 183 (1991) 89.
4. M. Dürr, A. Schmid, M. Obermaier, S. Rosselli, A. Yasuda, and G. Nelles, *Nature Materials*, 4 (2005) 607.
5. A. Fujishima and K. Honda, *Nature*, 238 (1972) 37.
6. M. R. Hoffmann, S. T. Martin, W. Choi, and D. W. Bahnemann, *Chemical Reviews*, 95 (1995) 69.
7. A. Kay and M. Grätzel, *Solar Energy Materials and Solar Cells*, 44 (1996) 99.
8. F. M. Hossain, L. Sheppard, J. Nowotny, and G. E. Murch, *Journal of Physics and Chemistry of Solids*, 69 (2008) 1820.
9. X. Chen and C. Burda, *Journal of the American Chemical Society*, 130 (2008) 5018.
10. A. Di Paola, M. Bellardita, and L. Palmisano, *Catalysts*, 3 (2013) 36.
11. M. Koelsch, S. Cassaignon, J. Guillemoles, and J. Jolivet, *Thin Solid Films*, 403 (2002) 312.
12. S.-D. Mo and W. Ching, *Physical Review B*, 51 (1995) 13023.
13. R. Dima, N. Maluta, R. Maphanga, and V. Sankaran, *Journal of Physics: Conference Series* (2017) 012012.
14. V. Binas, D. Venieri, D. Kotzias, and G. Kiriakidis, *Journal of Materiomics*, 3 (2017) 3.
15. F. De Angelis, S. Fantacci, A. Selloni, M. K. Nazeeruddin, and M. Grätzel, *The Journal of Physical Chemistry C*, 114 (2010) 6054.
16. T. Umabayashi, T. Yamaki, H. Itoh, and K. Asai, *Journal of Physics and Chemistry of Solids*, 63 (2002) 1909.
17. A. Di Paola G. Marci', L. Palmisano, M. Schiavello, K. Uosaki, S. Ikeda, and B. Ohtani, *The Journal of Physical Chemistry B*, 106 (2002) 106.
18. S.-m. Chang and R.-a. Doong, *The Journal of Physical Chemistry B*, 110 (2006) 20808.
19. Y. Segura, L. Chmielarz, P. Kustrowski, P. Cool, R. Dziembaj, and E. Vansant, *The Journal of Physical Chemistry B*, 110 (2006) 948.
20. B. Jongsomjit, T. Wongsalee, and P. Praserttham, *Catalysis Communications*, 6 (2005) 705.
21. K. Wilke and H. Breuer, *Journal of Photochemistry and Photobiology A: Chemistry*, 121 (1999) 49.
22. W. Choi, A. Termin, and M. R. Hoffmann, *The Journal of Physical Chemistry*, 98 (1994) 13669.
23. D. Dvoranova, V. Brezova, M. Mazúr, and M. A. Malati, *Applied Catalysis B: Environmental*, 37 (2002) 91.
24. S. U. Khan, M. Al-Shahry, and W. B. Ingler, *Science*, 297 (2002) 2243.
25. S. Sakthivel and H. Kisch, *Angewandte Chemie International Edition*, 42 (2003) 4908.
26. J. C. Yu, J. Yu, W. Ho, Z. Jiang, and L. Zhang, *Chemistry of Materials*, 14 (2002) 3808.
27. T. Umabayashi, T. Yamaki, S. Yamamoto, A. Miyashita, S. Tanaka, T. Sumita and K. Asai, *Journal of Applied Physics*, 93 (2003) 5156.
28. O. Diwald, T. L. Thompson, T. Zubkov, E. G. Goralski, S. D. Walck, and J. T. Yates, *The Journal*

- of *Physical Chemistry B*, 108 (2004) 6004.
29. M. Miyauchi, A. Ikezawa, H. Tobimatsu, H. Irie, and K. Hashimoto, *Physical Chemistry*, 6 (2004) 865.
 30. N. C. Saha and H. G. Tompkins, *Journal of Applied Physics*, 72 (1992) 3072.
 31. J. He, J. Zhao, T. Shen, H. Hidaka, and N. Serpone, *The Journal of Physical Chemistry B*, 101 (1997) 9027.
 32. A. Hattori, M. Yamamoto, H. Tada, and S. Ito, *Chemistry Letters*, 27 (1998) 707.
 33. K. M. Glassford and J. R. Chelikowsky, *Physical Review B*, 46 (1992) 1284.
 34. M. Landmann, E. Rauls, and W. Schmidt, *Journal of Physics: Condensed Matter*, 24 (2012) 195503.
 35. N. H. Vu, H. V. Le, T. M. Cao, V. V. Pham, H. M. Le, and D. Nguyen-Manh, *Journal of Physics: Condensed Matter*, 24 (2012) 405501.
 36. Z.-P. Liu, X.-Q. Gong, J. Kohanoff, C. Sanchez, and P. Hu, *Physical Review Letters*, 91 (2003) 266102.
 37. J. Muscat, V. Swamy, and N. M. Harrison, *Physical Review B*, 65 (2002) 224112.
 38. X. Wu, E. Holbig, and G. Steinle-Neumann, *Journal of Physics: Condensed Matter*, 22 (2010) 295501.
 39. A. R. Albuquerque, M. L. Garzim, I. d. M. d. Santos, V. Longo, E. Longo, and J. R. Sambrano, *The Journal of Physical Chemistry A*, 116 (2012) 11731.
 40. S. J. Clark, M. D. Segall, C. J. Pickard, P. J. Hasnip, M. J. Probert, K. Refson and M. C. Payne, *Zeitschrift Fuer Kristallographie*, 220 (2005) 567.
 41. A. Beltran, L. Gracia, and J. Andres, *The Journal of Physical Chemistry B*, 110 (2006) 23417.
 42. C. Dette, M. A. P. Osorio, C. S. Kley, P. Punke, C. E. Patrick, P. Jacobson, F. Giustino, S. J. Jung and K. Kern, *Nano Letters*, 14 (2014) 6533.
 43. S. Cataldo, B. M. Weckhuysen, A. Pettignano and B. Pignataro, *Catalysis Letters*, 148 (2018) 2459.
 44. H. Chen, X. Lia, R. Wan, S. K. Walter and Y. Lei, *Chemical Physics*, 501 (2017) 60.